



Alginate and Gum Arabic Coated Iron Oxide Nanoparticles as an Efficient Drug Carrier Agent

JAIVEER SINGH¹, ARTI JANGRA¹, KEERTI RANI¹, PARVIN KUMAR¹, SURESH KUMAR¹ and RAMESH KUMAR^{1*}

Department of Chemistry, Kurukshetra University, Kurukshetra-136119, India

*Corresponding author: E-mail: rameshkumarkuk@gmail.com

Received: 18 July 2021;

Accepted: 23 September 2021;

Published online: 16 December 2021;

AJC-20628

Multifunctional iron oxide nanoparticles have a vast and emerging scope in the field of nanotechnology. Out of numerous techniques available to develop multifunctional magnetite nanoparticles, co-precipitation is considered as one of the most efficient and economical techniques. Bare magnetite nanoparticles could be functionalized to act as multifunctional nanoparticles with the help of some suitable and biocompatible coating materials. In present study, surface functionalization of magnetic iron oxide nanoparticles has been carried out with alginate and gum Arabic, respectively. For the confirmation of surface functionalization, the synthesized multifunctional magnetite nanoparticles were characterized FTIR spectroscopy and thermogravimetric analysis. Further, the drug loading efficiency of these surface coated iron oxide nanoparticles has been evaluated with the help of UV-visible spectrophotometric studies.

Keywords: Iron oxide nanoparticles, Magnetite nanoparticles, Alginate, Gum Arabic, Cephalexin.

INTRODUCTION

Nanotechnology has played an indispensable role in the development of numerous fields of science. The versatility of nanotechnology has made it an unexampled and unmatched technique. Its role and importance could not be denied from the various fields of science. Among various nanomaterials, the multifunctional magnetite nanomaterials have a special importance due to their unique properties like high superparamagnetism, low toxicity and high biocompatibility with cells and tissues [1]. Magnetite nanoparticles are supposed to be one of the best non-toxic biocompatible drug carriers in the body of animals. Moreover, magnetite nanoparticles have a huge potential in the field of biomedical science starting from the process of recognition of the diseases (as MRI contrast agent) to the treatment of diseases (as drug carrier and hyperthermia agents) [2-4]. Interestingly, in some animals, nanocrystals of magnetite are found to act as magnetoreceptor. Magnetite nanoparticles are used for targeted drug delivery as these nanoparticles could be controlled with the help of magnetic field to direct the delivery of various drugs like anticancer drugs (doxorubicin) and antibiotics (cephalexin) to the specific site [5-7]. Magnetite nanoparticles, however,

tend to aggregate during their synthesis to reduce the surface energy.

To overcome this problem of agglomeration, the surface of bare magnetite nanoparticles has to be covered with appropriate surface coating agent. The ease of surface modification and the magnetic behaviour are dominating features of magnetite nanoparticles, which led these nanoparticles to be utilized in versatile ways. The surface of the magnetite nanoparticles can be modified with the help of polymeric moieties [8] oleic acid [9], chitosan [10], poly (vinyl alcohol) [11], poly(γ -glutamic acid) [12], etc. for their applications in various fields. It is the superparamagnetic behaviour of magnetite nanoparticles, which make them distinguished from non-magnetic nanoparticles for their use in biomedical arena. Due to this unique property, drug loaded magnetite nanoparticles can be directed to the tumor site with the help of external magnetic field [13-16]. Significant amount of work has been reported on magnetite nanoparticles for their applications in the field of biomedicine. Prompted by these applications, in the present article, magnetite nanoparticles coated with alginate and gum Arabic have been reported as an efficient drug loading agent. The materials selected for coating of bare magnetite nanoparticles are biocompatible, easy to store, non-immunogenic that makes them a potent choice for coating.

EXPERIMENTAL

All chemicals were of analytical grade and used without any further purification. Ferrous sulphate ($\text{FeSO}_4 \cdot 7\text{H}_2\text{O}$), ferric chloride ($\text{FeCl}_3 \cdot 6\text{H}_2\text{O}$), ammonium hydroxide and hydrochloric acid were purchased from SRL India. Sodium alginate and gum Arabic were purchased from CDH Fine Chemicals India. Deionized water was used throughout the experiments.

T90 PG Instrument Limited UV-vis spectrometer (900-190 nm), Shimadzu RF-5301 PC spectrofluorometer, Rigaku Ultima IV fully automatic high resolution X-Ray Diffractometer system with theta-theta goniometer, Philips CM 200 transmission electron microscope, MB-3000 ABB spectrophotometer (KBr pellets). Digital Laboratory stirrer (Popular Trader, India).

Synthesis of bare magnetite nanoparticles: Magnetite nanoparticles were synthesized by alkaline co-precipitation of ferric chloride ($\text{FeCl}_3 \cdot 6\text{H}_2\text{O}$) and ferrous sulphate ($\text{FeSO}_4 \cdot 7\text{H}_2\text{O}$) in a molar ratio of 2:1. The reaction mixture was stirred in a glass vessel with an agitation rate of 2200 rpm under inert atmosphere (N_2 gas). During the reaction, temperature was maintained between 85-90 °C. After that 20 mL of ammonium hydroxide, saturated with N_2 gas for 30 min, was added to the reaction mixture dropwise to raise the pH ~ 9-10. Black coloured iron oxide nanoparticles were formed. The black precipitate was stirred further for a period of 30 min and then washed several times with deionized water. The bare magnetite nanoparticles were dried in vacuum oven at 25 °C.

Surface functionalization of magnetite nanoparticles

Gum Arabic functionalized magnetite nanoparticles (GA@MNPs): For surface functionalization, black coloured bare magnetite nanoparticles were precipitated as discussed above. To the stirring reaction mixture containing black precipitate of iron oxide nanoparticles was added 20 mL of aqueous solution of gum Arabic was added. The stirring was further continued for 2 h under nitrogen atmosphere. The resulting surface functionalized magnetite nanoparticles were isolated and used for drug loading studies.

Alginate functionalized magnetite nanoparticles (AA@MNPs): The alginate functionalized magnetite nanoparticles were synthesized by adopting the same procedure used for surface functionalization of magnetite nanoparticles with gum Arabic. However, in this case coating material used was sodium alginate instead of gum Arabic. The alginate functionalized magnetite nanoparticles were also used for drug loading studies.

Drug loading on AA@MNPs and GA@MNP: For the loading of drug on the surface functionalized magnetite nanoparticles, 1 g of functionalized magnetite nanoparticles was dispersed in 50 mL of deionized water with the help of probe sonicator for 10 min. Similarly, varying amount of cephalixin drug (10-100 mg) was also dispersed in 50 mL deionized water with the help of probe sonicator for 10 min. Now, the former solution was set into rotary shaker (200 rpm) and the later drug solution was added slowly to this solution and shaken continuously at a rate of 200 rpm for 24 h at room temperature. After that the resultant mixture was centrifuged for 10 min and the supernatant was carefully separated from the precipitate

for the study of drug entrapment efficiency using UV visible spectrophotometer.

Drug entrapment efficiency: The drug entrapment efficiency was determined by measuring the amount of free drug present in the supernatant by UV-visible spectroscopy at calibrated wavelength ($\lambda_{\text{max}} = 293 \text{ nm}$) in UV-visible spectrophotometer. Drug entrapment efficiency was calculated by following formula:

$$\text{Entrapment efficiency (\%)} = \frac{\text{Total amount of drug} - \text{Free drug in supernatant}}{\text{Total amount of drug}} \times 100$$

Characterization of bare and surface functionalized MNPs (GA@MNPs and AA@MNPs): The surface functionalization of magnetite nanoparticles with the coating agents gum Arabic and alginate was confirmed with the help of FTIR studies. For this purpose, the FTIR spectrum of bare MNPs was compared with IR spectra of GA@MNPs and AA@MNPs. The XRD studies were performed to examine the crystalline properties of functionalized nanoparticles as well as to confirm the presence of pure phase of magnetite. The highly crystalline nature of functionalized nanoparticles was confirmed by the presence of sharp and intense peaks in the X-ray diffractogram. Moreover, the morphological analysis of surface functionalized magnetite nanoparticles was carried out with the help of transmission electron microscope. Further, the impact of surface coating on the diameters of nanoparticles was also observed by comparing the TEM images of bare and surface coated nanoparticles. The thermogravimetric studies were carried out in the temperature range between 25 to 700 °C at a heating rate of 10 °C min^{-1} under the N_2 atmosphere. For the investigation of the magnetic behaviour of the bare and surface modified magnetite nanoparticles, VSM studies were carried out. The magnetic saturation value was determined by plotting the extrapolation curves. The impact of surface functionalization was also observed by the comparative study of the VSM plots of bare and coated magnetite nanoparticles (AA@MNPs and GA@MNPs).

RESULTS AND DISCUSSION

FTIR spectral studies of bare and AA@MNPs: A sharp peak near 600 cm^{-1} , corresponding to Fe-O stretching vibration is common in IR spectra of bare magnetite nanoparticles and AA@MNPs. IR spectrum of pure sodium alginate powder showed two medium intensity peaks near 1413 and 1586 cm^{-1} that may be assigned to asymmetric and symmetric stretching of carboxylate ion [17]. These peaks were also observed in the IR spectrum of AA@MNPs. Further, a broad peak at 3340 cm^{-1} and another peak at 1021 cm^{-1} arise due to O-H stretch and C-O stretch, respectively [18] in IR spectra of pure alginate powder as well as alginate functionalized magnetite nanoparticles. Thus, the comparative studies of FTIR spectra of bare magnetite nanoparticles (Fig. 1a), pure alginate (Fig. 1b) and alginate functionalized magnetite nanoparticles (Fig. 1c) have confirmed the successful surface coating of magnetite nanoparticles with alginate.

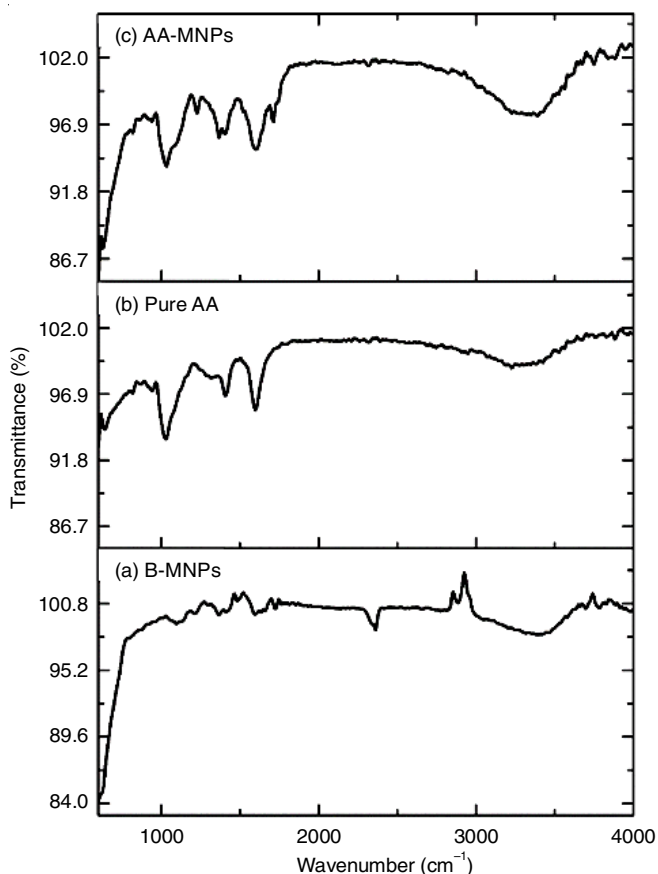


Fig. 1. FTIR spectrum of (a) bare magnetite nanoparticles, (b) pure alginate (c) alginate functionalized magnetite nanoparticles

FTIR spectral studies of bare and GA@MNPs: FTIR spectrum of pure gum Arabic powder showed peaks related to carboxylate asymmetric and symmetric stretch at 1431 and 1613 cm^{-1} [19]. Gum Arabic contains high molecular weight glycoprotein and low molecular weight polysaccharide in high percentage giving rise to peaks corresponding to N-H stretch (primary and secondary) and O-H stretch, respectively, in the region 3500-3200 cm^{-1} . The peaks obtained due to N-H stretch and O-H stretch are overlapped being present in the same region and cannot be assigned individually [20]. The peaks observed at 1045 and 1295 cm^{-1} may be attributed to C-O and C-N stretching, respectively [21,22]. The similar peaks have also been observed in the IR spectrum of gum Arabic coated magnetite nanoparticles. Thus, the comparison of FTIR spectrum of bare magnetite nanoparticles (Fig. 2a) with the FTIR spectra of pure gum Arabic powder (Fig. 2b) and gum Arabic functionalized magnetite nanoparticles (Fig. 2c) gave an idea that surface of bare magnetite nanoparticles has been modified with gum Arabic.

TEM studies: Particle size and morphology of bare as well as surface functionalized magnetite nanoparticles (AA@MNPs and GA@MNPs) were analyzed by TEM. TEM images of bare MNPs, alginate modified magnetite nanoparticles and gum-Arabic modified magnetite nanoparticles are represented in Fig. 3a-c, respectively. The TEM images showed that the shape of nanoparticles is almost spherical. The average particle size for the bare magnetite nanoparticles was found to be 10

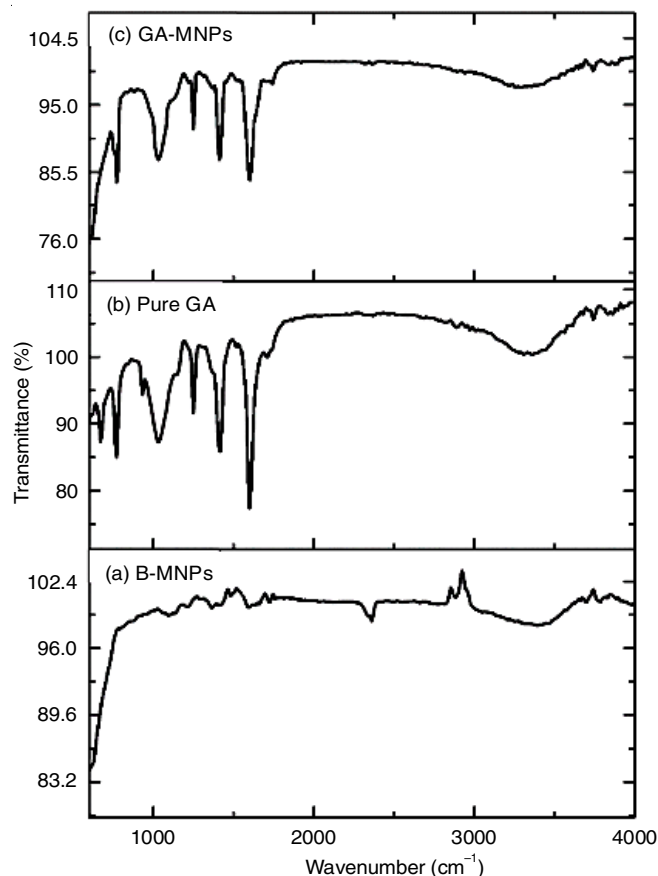


Fig. 2. FTIR spectrum of (a) bare magnetite nanoparticles, (b) pure gum Arabic, (c) gum arabic functionalized magnetite nanoparticles

nm, which is very close to already reported values for the bare magnetite nanoparticles. The average size of the surface functionalized nanoparticles was found to be increased slightly as per the expectations.

XRD studies: The crystalline structure of the magnetite nanoparticles was confirmed by X-ray diffraction (XRD) technique at room temperature (298 K). The XRD spectra showed common diffraction peaks for both bare MNPs (Fig. 4a) and surface functionalized MNPs (AA@MNPs; Fig. 4b and GA@MNPs; Fig. 4c) revealing that crystal structure of core MNPs is not affected even after surface functionalization of bare MNPs. Moreover, the XRD pattern of bare and coated MNPs confirmed that these nanoparticles have inverse type spinel structure.

TGA studies: Thermograms of bare MNPs and surface functionalized MNPs were obtained by heating them up to 700 $^{\circ}\text{C}$ under nitrogen atmosphere. Comparative studies of the thermogram of bare and surface functionalized nanoparticles helped to confirm the successful coating of alginate and gum Arabic on the surface of magnetite nanoparticles. A close investigation of the thermograms and three-phase thermal degradation gave an idea about the extent of coating on the Fe_3O_4 nanoparticle surface. From the thermogram of AA@MNPs, It can be concluded that around 8% weight loss observed in the first step (25-200 $^{\circ}\text{C}$) may be attributed to the loss of absorbed moisture. In the second step (200-450 $^{\circ}\text{C}$), weight loss of about 40% was observed, which may be assigned to second stage thermal degradation and this dip in the thermogram

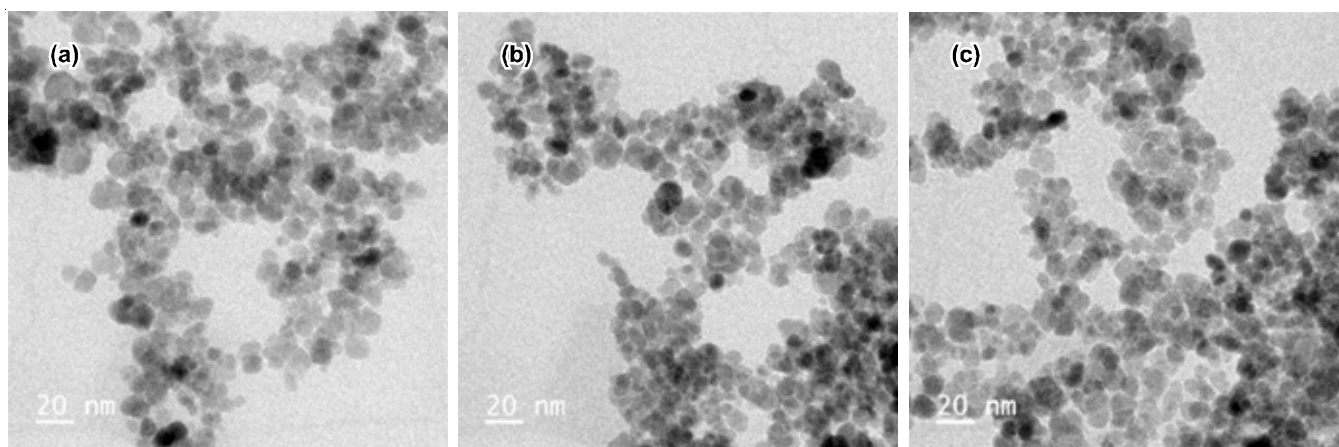


Fig. 3. TEM images of (a) bare magnetite nanoparticles, (b) alginate functionalized magnetite nanoparticles, (c) gum arabic functionalized magnetite nanoparticles

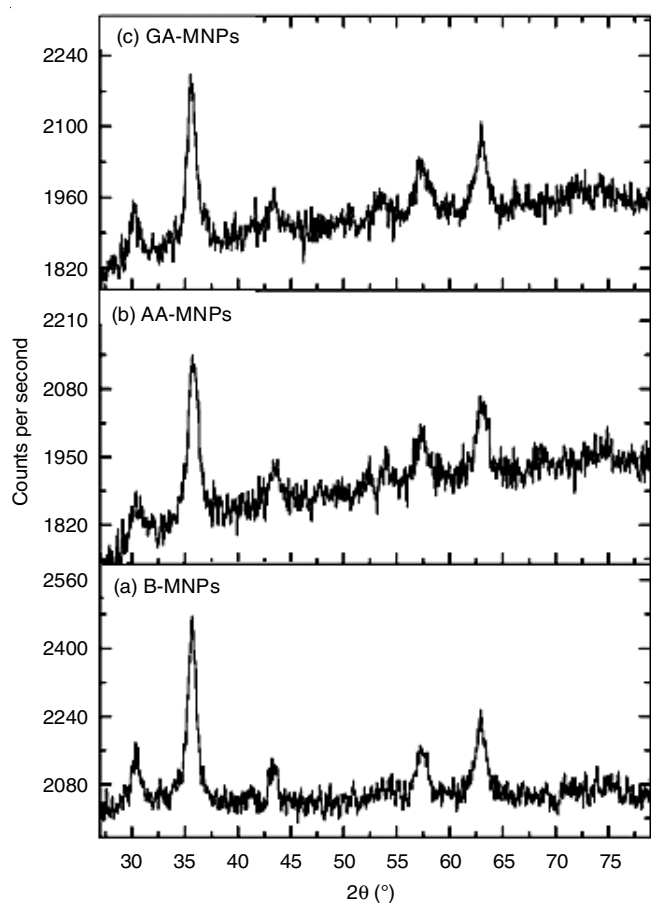


Fig. 4. XRD plot of (a) bare magnetite nanoparticles, (b) alginate functionalized magnetite nanoparticles, (c) gum arabic functionalized magnetite nanoparticles

is supposed to be due to the degradation of coating material *i.e.* sodium alginate present on surface of Fe_3O_4 nanoparticles [23]. The weight loss of about 1%, in the third step (500-660 °C) corresponds to the decay of sodium alginate residues. Therefore, in thermogram of AA@MNPs the three-phase degradation is observed mainly due to degradation of organic moiety *i.e.* alginate coated on the surface of magnetite nanoparticles. Further, it was concluded that the coating is quite

stable upto 210 °C and hence can be used upto this temperature limit for further applications. Similarly, from the thermogram of GA@MNPs, three phases of weight loss were found to signify the successful surface functionalization of magnetite nanoparticles with gum Arabic. A weight loss about 5% was observed in the first phase (25-200 °C), due to moisture loss. In the second phase (200-420 °C), about 25% weight loss was observed owing to decomposition of gum Arabic coating from the surface of magnetite nanoparticles [24]. In the third phase (450-650 °C), a weight loss of about 1% was observed which may be assigned to the decomposition of gum Arabic residue. Hence from these observations, it can be safely concluded that the surface of the bare magnetite nanoparticles is successfully covered with the coating agent.

VSM studies: The comparison of magnetization curve of bare MNPs (Fig. 5a) with the magnetization curve of the surface functionalized magnetite nanoparticles AA@MNPs (Fig. 5b) and GA@MNPs (Fig. 5c), illustrate the change in magnetic properties of bare magnetite nanoparticles after coating of alginate and gum Arabic, respectively on its surface. The superparamagnetic behaviour of the bare and coated magnetite nanoparticles was evident from their magnetization curves (Fig. 5a-c) as the M-H curve in each case has shown negligible coercivity (H_c) and remanence (M_r) value at room temperature. The saturation magnetization value (M_s) was calculated by the extrapolation of M vs. $1/H$ curve. The M_s value of bare MNPs, gum Arabic functionalized and alginate functionalized magnetite nanoparticles were found to be 1.749, 1.680 and 0.907 emu/g, respectively (Fig. 6). A decrease in the M_s value was observed for the surface functionalized nanoparticles as compared to bare magnetite nanoparticles that could be possibly due to the disruption of long-range order magnetic exchange interaction on the outer surface of nanoparticle [25]. From the magnetic data, the magnetic susceptibility value of bare and coated magnetite nanoparticles (AA@MNPs and GA@MNPs) was calculated from the differential susceptibility curve (Fig. 7)

i.e. d_M/d_H vs. H . The magnetic susceptibility *i.e.* $\chi_i = \left(\frac{d_M}{d_H} \right)_{H \rightarrow 0}$ of bare, gum Arabic functionalized and alginate functionalized

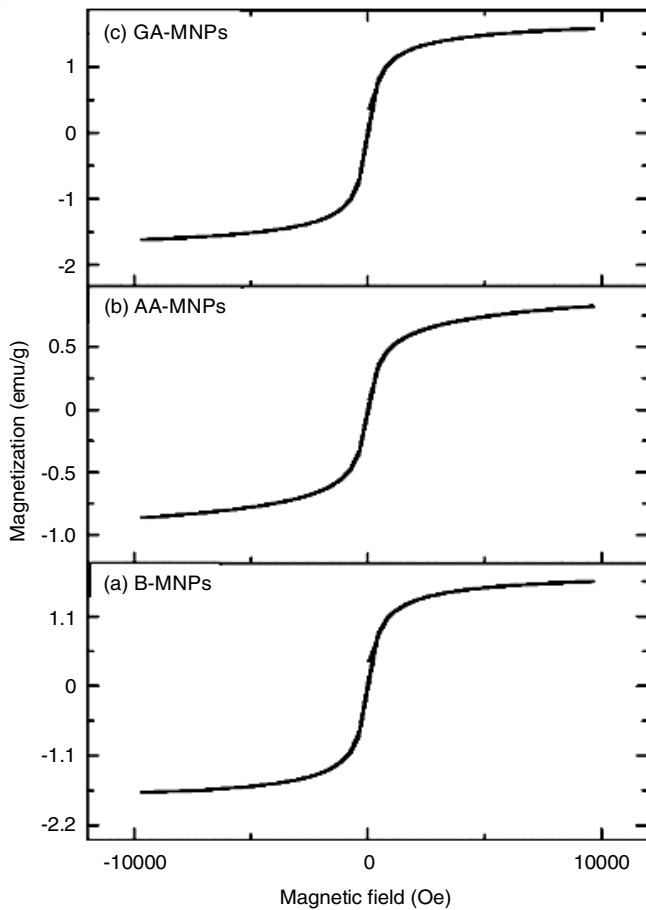


Fig. 5. VSM plots of (a) bare magnetite nanoparticles, (b) alginate functionalized magnetite nanoparticles, (c) gum Arabic functionalized magnetite nanoparticles

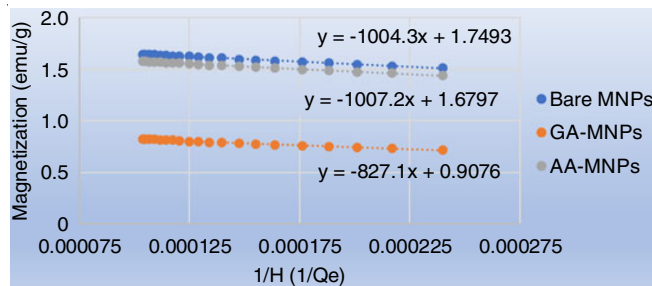


Fig. 6. Plot of magnetization value (emu/g) versus 1/H (1/Oe) of bare, alginate functionalized and gum Arabic functionalized magnetite nanoparticles for the determination of saturation magnetization

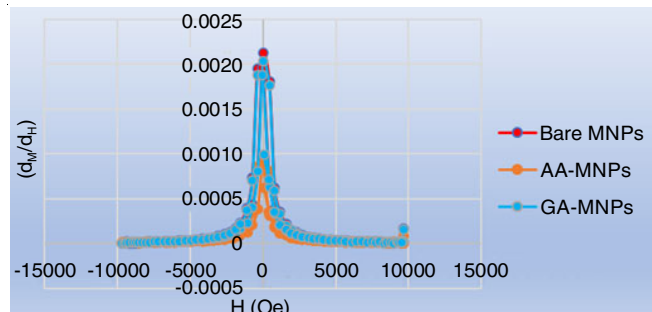


Fig. 7. Differential susceptibility curve of bare, alginate functionalized and gum Arabic functionalized magnetite nanoparticles for the determination of magnetic susceptibility

nanoparticles were found to be 2.1×10^{-3} , 2.0×10^{-3} and 9.1×10^{-4} , respectively (Table-1).

Sample	χ_i^a	M_s (emu/g) ^b	H_c (Oe) ^c	M_r (emu/g) ^d
Bare MNPs	2.1×10^{-3}	1.749	0	0
AA@MNPs	9.1×10^{-4}	0.907	0	0
GA@MNPs	2.0×10^{-3}	1.680	0	0

where, ^aMagnetic susceptibility (degree of magnetization of nanoparticles in response to applied magnetic field); ^bSaturation magnetization (maximum possible magnetization); ^cCoercivity (intensity of the applied magnetic field required to reduce the magnetization of nanoparticles to zero); ^dRemanence (magnetization left in nanoparticles when external magnetic field is removed).

Loading of cephalexin drug on AA@MNPs and GA@MNPs: The calibration curve of drug was plotted by using 10 times dilution factor (Fig. 8) and the calculated λ_{max} for cephalexin drug was found to be 520 nm. The supernatant was obtained and diluted to 100 times to determine the drug concentration using a UV-vis spectrophotometer at 520 nm. The efficiency of the adsorption of the cephalexin drug by the surface functionalized magnetite nanoparticles (AA@MNPs and GA@MNPs) was analyzed with the help of two parameters *i.e.* adsorption capacity of the adsorbent denoted by q_t (mg/g) and the percentage removal of the adsorbate denoted by %R, the expression as shown in eqns. 1 and 2, respectively [26,27].

$$q_t = \frac{C_i - C_f}{W} \times V \tag{1}$$

$$R (\%) = \frac{C_i - C_e}{C_i} \times 100 \tag{2}$$

where, C_i , C_f and C_e represents the initial, final and equilibrium concentration of the drug in the aqueous phase (mg/L), respectively, V is the volume of the drug solution (L) and W represents the quantity of the adsorbent (g).

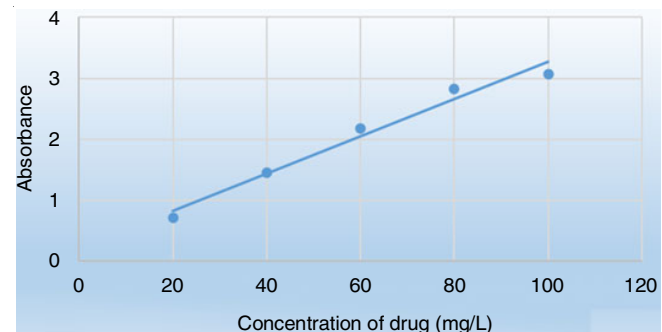


Fig. 8. Calibration curve for cephalexin drug

Cephalexin drug loading study: The cephalexin drug loading profile of alginate and gum Arabic coated iron oxide nanoparticle carriers are shown in Figs. 9 and 10, respectively. The process of adsorption of cephalexin drug on surface functionalized magnetite nanoparticles follows a pattern of initially a rapid adsorption process followed by the slowdown of the

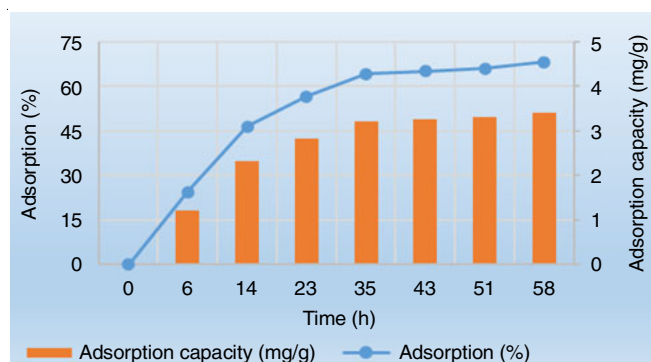


Fig. 9. Drug loading profile of alginate coated magnetite nanoparticles

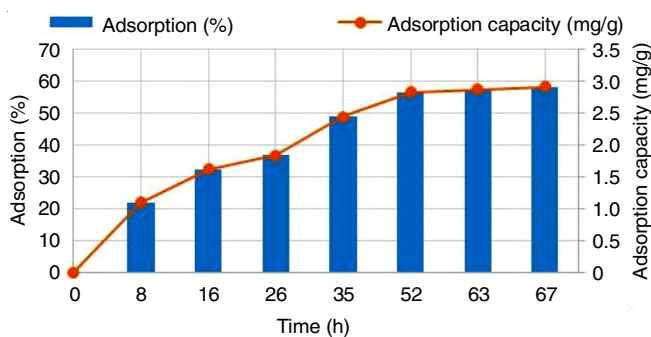


Fig. 10. Drug loading profile of gum Arabic coated magnetite nanoparticles

adsorption process and finally reaches to the saturation value. The approximate equilibrium time for the adsorption of cephalexin drug on AA@MNPs has been found 35 h while for GA@MNPs, it was found to be 52 h. The maximum value of entrapment efficiency for alginate functionalized magnetite nanoparticles (AA@MNP) was found to be around 65% at 50 mg/L drug concentration. However, for gum Arabic functionalized magnetite nanoparticles (GA@MNP) it was found to be around 58% at 60 mg/L drug concentration. The effect of initial concentration of drug on the adsorption behaviour of cephalexin drug on the alginate and gum Arabic functionalized magnetite nanoparticles are shown in Figs. 11 and 12, respectively. The presence of larger uncovered surface area on the adsorbent and greater concentration gradient in the beginning of the adsorption process acts as major factor in the rapid adsorption of the drug [28]. Afterward, the drug entered into the pores and the adsorption process slows down due to the slow pore diffusion of the drug molecules into the adsorbent bulk [29].

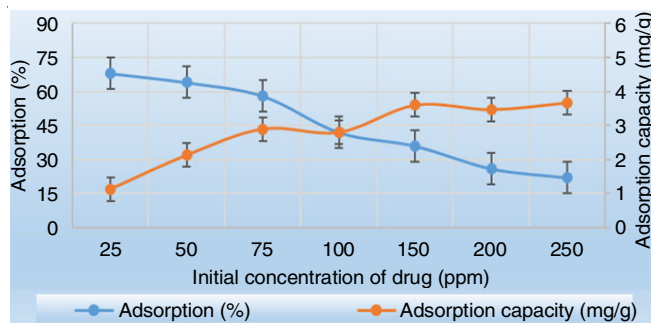


Fig. 11. Effect of initial concentration of drug on the adsorption of drug by alginate functionalized magnetite nanoparticles

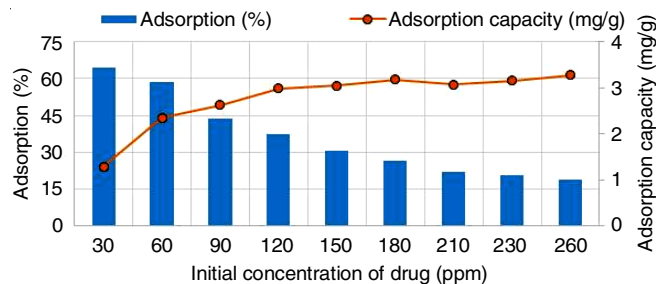


Fig. 12. Effect of initial concentration of drug on the adsorption of drug by gum Arabic functionalized magnetite nanoparticles

Cephalexin drug release from the drug loaded surface functionalized magnetite nanoparticles: The drug release behaviour has a potential significance in the targeted drug delivery and is an important factor for analyzing the reusability of the adsorbent. The release of a drug from the adsorbent is highly dependent on the fluid used for the desorption of the drug from the adsorbent. The fluid must penetrate into the pores or the chains present on the surface of the adsorbent. For better result of drug release from the surface of nanoparticles, the drug must get dissolved into the permeating fluid so that it may be easily diffused from the surface on which it is adsorbed [30,31]. Beside this, change in the pH of the solution may also play important role in release of drug from coated magnetite nanoparticles. In present study, the optimized pH was determined for maximum amount of drug release and found that best results for the release of cephalexin drug from alginate functionalized and gum Arabic functionalized magnetite nanoparticles were obtained at pH 9 and 10, respectively (Fig. 13). It was also observed that a maximum of 80% drug was released from the surface of alginate functionalized magnetite nanoparticles after a period of 32 h. However, in case of gum Arabic functionalized magnetite nanoparticles a maximum of 60% drug was released but it took 25 h (Fig. 13). So, it is evident that AA@MNPs and GA@MNPs may be used as a potential drug carrier and can be reused after desorption of drug from their surface.

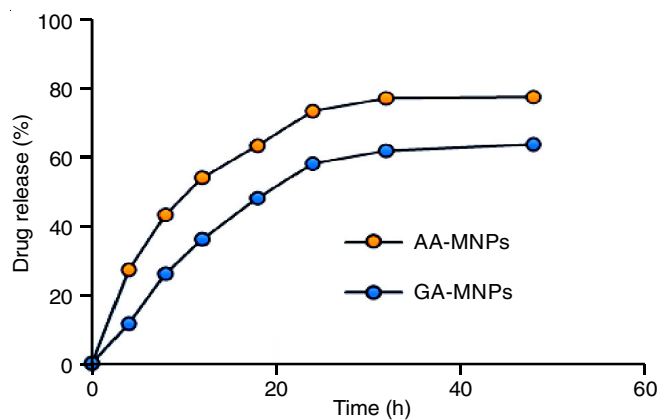


Fig. 13. Drug release profile of alginate and gum Arabic coated magnetite nanoparticles

Conclusion

The magnetite nanoparticles synthesized by a facile chemical coprecipitation technique were stabilized and surface

functionalized using non-toxic and biocompatible polymers *i.e.* sodium alginate and gum Arabic. XRD, FTIR, TEM, TGA and VSM techniques were used for the characterization of bare and surface functionalized magnetite nanoparticles. FTIR and TGA techniques confirmed the successful coating of both the coating agents (alginate and gum Arabic) onto the surface of magnetite nanoparticles. The VSM results interpreted the minor decrease in magnetization saturation value of the coated nanoparticles as compared to bare magnetite nanoparticles. Further, AA@MNPs and GA@MNPs were used as drug loading agents. The loading capacity of cephalexin drug on surface of functionalized magnetite nanoparticles has been found to be increased with the contact time. Beside this, drug release studies revealed that drug loaded on the surface of surface modified magnetite nanoparticles can be successfully released under certain optimized conditions. In nutshell, it may be concluded that alginate as well as gum Arabic functionalized magnetite nanoparticles can be efficiently used as potential cephalexin drug carrier.

ACKNOWLEDGEMENTS

One of the authors, Jaiveer Singh is thankful for the financial support provided by UGC, New Delhi (India) in the form of SRF and Department of Chemistry, Kurukshetra University, Kurukshetra (India) for providing the research facilities.

CONFLICT OF INTEREST

The authors declare that there is no conflict of interests regarding the publication of this article.

REFERENCES

- S. Gul, S.B. Khan, I.U. Rehman, M.A. Khan and M.I. Khan, *Front. Mater.*, **6**, 179 (2019); <https://doi.org/10.3389/fmats.2019.00179>
- J. Estelrich, E. Escibano, J. Queralt and M.A. Busquets, *Int. J. Mol. Sci.*, **16**, 8070 (2015); <https://doi.org/10.3390/ijms16048070>
- S. Natarajan, K. Harini, G.P. Gajula, B. Sarmento, M.T. Neves-Petersen and V. Thiagarajan, *BMC Mater.*, **1**, 2 (2019); <https://doi.org/10.1186/s42833-019-0002-6>
- L. Zhang, F. Yu, A.J. Cole, B. Chertok, A.E. David, J. Wang and V.C. Yang, *AAPS J.*, **11**, 693 (2009); <https://doi.org/10.1208/s12248-009-9151-y>
- Y.P. Yew, K. Shameli, M. Miyake, N.B.B. Ahmad Khairudin, S.E.B. Mohamad, T. Naiki and K.X. Lee, *Arab. J. Chem.*, **13**, 2287 (2020); <https://doi.org/10.1016/j.arabjc.2018.04.013>
- M. Patitsa, K. Karathanou, Z. Kanaki, L. Tzioga, N. Pippa, C. Demetzos, D.A. Verganelakis, Z. Cournia and A. Klinakis, *Sci. Rep.*, **7**, 775 (2017); <https://doi.org/10.1038/s41598-017-00836-y>
- S. Sirivisoot and B.S. Harrison, *Int. J. Nanomedicine*, **10**, 4447 (2015); <https://doi.org/10.2147/IJN.S82830>
- W. Wu, Z. Wu, T. Yu, C. Jiang and W.S. Kim, *Sci. Technol. Adv. Mater.*, **16**, 023501 (2015); <https://doi.org/10.1088/1468-6996/16/2/023501>
- N.W. Bolden, V. Rangari and S. Jeelani, In ICCM-17-17th International Conference on Composite Materials (2009).
- S. Kariminia, A. Shamsipur and M. Shamsipur, *J. Pharm. Biomed. Anal.*, **129**, 450 (2016); <https://doi.org/10.1016/j.jpba.2016.07.016>
- T.D. Nguyen, S.T. Vo, V.T. Thanh Ho, X.T. Le and L.G. Bach, *Asian J. Chem.*, **30**, 1711 (2018); <https://doi.org/10.14233/ajchem.2018.21245>
- R. Kumar, B.S. Inbaraj and B.H. Chen, *Mater. Res. Bull.*, **45**, 1603 (2010); <https://doi.org/10.1016/j.materresbull.2010.07.017>
- R. Sivashankar, A.B. Sathya, K. Vasantharaj and V. Sivasubramanian, *Environ. Nanotechnol. Monit. Manag.*, **1-2**, 36 (2014); <https://doi.org/10.1016/j.enmm.2014.06.001>
- Z. Durmus, H. Sözeri, B. Unal, A. Baykal, R. Topkaya, S. Kazan and M.S. Toprak, *Polyhedron*, **30**, 322 (2011); <https://doi.org/10.1016/j.poly.2010.10.028>
- L. Zhang, F. Yu, A.J. Cole, B. Chertok, A.E. David, J. Wang and V.C. Yang, *AAPS J.*, **11**, 693 (2009); <https://doi.org/10.1208/s12248-009-9151-y>
- D.T. Nguyen, P.T. Nhan Nguyen, T.H. Tran, D.H. Nguyen, D.V. N. Vo, M.R. Islam, K.T. Lim, S.T. Vo and L.G. Bach, *Asian J. Chem.*, **31**, 767 (2019); <https://doi.org/10.14233/ajchem.2019.21617>
- M. Sivagnanavelmurugan, S. Radhakrishnan, A. Palavesam, V. Arul and G. Immanuel, *Int. J. Curr. Res. Life Sci.*, **7**, 1863 (2018).
- J.A. Lozano-Alvarez, J. Jauregui-Rincon, G. Mendoza-Diaz, R. Rodriguez-Vazquez and C. Frausto-Reyes, *J. Mex. Chem. Soc.*, **53**, 59 (2009).
- C.A. Ibeke, G.M. Oyatogun, T.A. Esan and K.M. Oluwasegun, *Am. J. Mater. Sci.*, **5**, 28 (2017); <https://doi.org/10.12691/ajmse-5-1-4>
- M. Eskandari-Nojehdehi, H. Jafarizadeh-Malmiri and A. Jafarizad, *Z. Phys. Chem.*, **232**, 325 (2018); <https://doi.org/10.1515/zpch-2017-1001>
- R.M.A. Daoub, A.H. Elmubarak, M. Misran, E.A. Hassan and M.E. Osman, *J. Saudi Soc. Agric. Sci.*, **17**, 241 (2018); <https://doi.org/10.1016/j.jssas.2016.05.002>
- C. Cai, R. Ma, M. Duan and D. Lu, *RSC Advances*, **9**, 19740 (2019); <https://doi.org/10.1039/C9RA03323H>
- E.Y. Ionashiro, T.S.R. Hower, F.L. Ferttonani, E.T. Almeida and M. Ionashiro, *Ecl. Quím. J.*, **29**, 53 (2004); <https://doi.org/10.1590/S0100-46702004000200008>
- C.G. Mothe and M.A. Rao, *Thermochim. Acta*, **357-358**, 9 (2000); [https://doi.org/10.1016/S0040-6031\(00\)00358-0](https://doi.org/10.1016/S0040-6031(00)00358-0)
- P.T.M. Huong, T.A. Thu, C.Q. Thuong, T.H. Con and N.T. Huong, *Asian J. Chem.*, **32**, 602 (2020); <https://doi.org/10.14233/ajchem.2020.22455>
- A.A. Mohammed, T.J. Al-Musawi, S.L. Kareem, M. Zarrabi and A.M. Al-Ma'abreh, *Arab. J. Chem.*, **13**, 4629 (2020); <https://doi.org/10.1016/j.arabjc.2019.10.010>
- Z.H. Xing, *Asian J. Chem.*, **25**, 9532 (2013); <https://doi.org/10.14233/ajchem.2013.15066>
- A. Mohseni Bandpi, T.J. Al-Musawi, E. Ghahramani, M. Zarrabi, S. Mohebi and S.A. Vahed, *J. Mol. Liq.*, **218**, 615 (2016); <https://doi.org/10.1016/j.molliq.2016.02.092>
- A. Fakhri and S. Adami, *J. Taiwan Inst. Chem. Eng.*, **45**, 1001 (2014); <https://doi.org/10.1016/j.jtice.2013.09.028>
- A. Nezamzadeh-Ejhieh and S. Tavakoli-Ghinani, *C.R. Chim.*, **17**, 49 (2014); <https://doi.org/10.1016/j.crci.2013.07.009>
- A. Lajvardi, M. Hossaini Sadr, M. Tavakkoli Yarak, A. Badiei and M. Armaghan, *New J. Chem.*, **42**, 9690 (2018); <https://doi.org/10.1039/C8NJ01375F>